https://doi.org/10.2352/ISSN.2470-1173.2020.14.COIMG-059

Single-shot Coded Diffraction System for 3D Object Shape Estimation

Samuel Pinilla[1] ***; Laura Galvis***[1] ***; Karen Egiazarian***[2] ***; Henry Arguello***[1]
[1] ***Universidad Industrial de Santander, Bucaramanga, Colombia.***
[2] ***Tampere University, Tampere, Finland.***

Abstract

The three-dimensional (3D) shape reconstruction problem of an object is a task of high interest in autonomous vehicles, detection of moving objects, and precision agriculture. A common methodology to recover the 3D shape of an object is using its optical phase. However, this approach involves solving a non-convex computationally demanding inverse problem known as phase retrieval (PR) in a setup that records coded diffraction patterns (CDP). Usually, the acquisition of several snapshots from the scene is required to solve the PR problem. This work proposes a single-shot 3D shape estimation technique using the optical phase of the object from CDP. The presented approach consists on accurately estimating the optical phase of the object by low-pass-filtering the leading eigenvector of a carefully constructed matrix. Then, the estimated phase is used to infer the 3D object shape. It is important to mention that the estimation procedure does not involve a full time demanding reconstruction of the objects. Numerical results on synthetic data demonstrate that the proposed methodology closely estimates the 3D surface of an object with a normalized Mean-Square-Error of up to 0.27, under both noiseless and noisy scenarios. Additionally, the proposed method requires up to 60% less measurements to accurately estimate the 3D surface compared to a state-of-the-art methodology.

Introduction

The task of reconstructing the three-dimensional (3D) shape of an object is one of the most studied problems in computer vision. Many techniques have been developed in the state-of-the-art to solve this problem including light field [1], point cloud images [2], using collection of images [3], and structured light [4], among others [5, 6, 7, 8, 9, 10]. In the state-of-the-art several descriptors haven been used for the aforementioned techniques to reconstruct the 3D surface including the epipolar plane for the case of light field [2], inferring local correspondences on matched images [3], and the optical phase of the object in structured light [2, 4]. This work focuses on the estimation of the 3D object shape using its optical phase information. Compared with the remainder strategies in the state-of-the-art and, since it is a non-contact technique, it requires less running time and measurements to obtain the 3D object shape.

There are two possibilities to estimate the 3D object surface from its optical phase, first through structure light and second solving a phase retrieval (PR) problem. For the first case, shape reconstruction algorithms are divided into two categories: multi-shot [5, 6] and single-shot [8, 9]. Multi-shot methods can estimate the per-pixel depth map for a wide range of objects using temporal coding of the illumination patterns but require the scene to be stationary during image acquisition. Additionally, since several snapshots have to be acquired, the sensing and running time to reconstruct the 3D object shape is larger compared with single-shot methods. Particularly, the most recent single-shot strategy introduced in [2] projects an array of narrow lines into the 3D object, and the reflection of this interaction is then acquired with two cameras. The two acquired images are combined using a triangulation methodology to obtain the phase of the object and, therefore its 3D shape. The main disadvantage of [2] compared with the alternatives in the state-of-the-art, is that it requires the two images to resolve around 3×10^5 points to reconstruct the 3D shape of the object more accurately, which implies higher computational complexity.

An alternative path to estimate the optical phase of a 3D object is by solving the PR problem in a setup that records coded diffraction patterns (CDP) [11, 12, 13]. Several PR algorithms have been proposed to recover the phase information given CDP. In particular, PR algorithms are based on alternating minimization [14], convex programming [15], non-convex minimization using a stochastic smoothing function [16], matrix completion [13], sparsity using quadratic compressed sensing [17], and wirtinger flow [18]. More recent methods include the truncated amplitude flow (TAF) [19], reweighted amplitude flow (RAF) [20], and truncated wirtinger flow (TWF) [21]. One of the critical stages of the aforementioned algorithms that solve the PR problem is the estimation of an initial guess. To this end, several strategies have been proposed in PR, such as orthogonality-promoting initialization [19], weighted maximal correlation initialization [20], and truncated spectral initialization [21]. These methods estimate the object without reconstructing the image.

The main disadvantage of the PR-based strategy is that it is a computationally demanding non-convex problem, that constitutes an instance of non-convex quadratic programming [22]. One possibility to avoid full-time reconstruction in PR is the use of initialization methods that can be used to estimate the optical phase of the object. However, these initialization approaches require a large number of measurements to achieve a proper estimation of the scene for both noiseless and noisy scenarios, which implies more processing time, as numerically illustrated the numerical results section.

This work proposes a single-shot 3D shape estimation technique using the optical phase of the object from CDP. The presented approach consists of accurately estimating the optical phase of the object by low-pass-filtering the leading eigenvector of a carefully constructed matrix. Then, the estimated phase is used to infer the 3D object shape. It is important to mention that the estimation procedure does not involve a full time demanding

reconstruction of the objects. Numerical results on synthetic data demonstrate that the proposed methodology closely estimates the 3D surface of an object with a normalized Mean-Square-Error of up to 0.27, under both noiseless and noisy scenarios. The traditional initialization techniques tend to return inaccurate estimations of the phase when the measurements are corrupted by noise compared to the proposed estimation method. Additionally, the proposed method requires up to 75% and 60% fewer measurements to accurately estimate the phase and the 3D surface, compared to the state-of-the-art strategies and a structured light methodology, respectively.

Coded Acquisition System

This section introduces the optical system that collects a CDP of a scene, as illustrated in Fig. 1. In contrast to state-of-the-art optical setups, this architecture allows the reconstruction of the optical phase of an object from the acquired CDP [23].

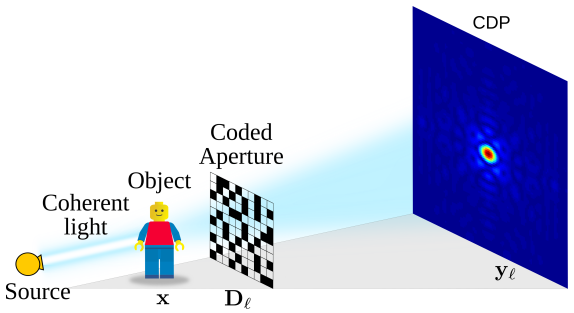

Figure 1. *Schematic representation of an optical system that acquires CDP. At the ℓ-th snapshot, a coded aperture $\mathbf{D}_\ell$ is introduced between the object $\mathbf{x}$ and the sensor to modulate the input field.*

Notice that the optical system illustrated in Fig. 1 includes a coded aperture between the object of interest and the sensor. This coded aperture modulates the signal before being finally measured at the intensity array detector. There are several ways of achieving modulations of this type: using a phase mask, or using an optical grating to modulate the illumination beam as mentioned in [24], or even by techniques from ptychography which scan an illumination patch on an extended specimen [25, 26]. Additionally, by changing the spatial configuration of the coded aperture, this acquisition system allows capturing multiple snapshots of the scene.

Mathematically, the acquisition process of the ℓ-th snapshot by the system illustrated in Fig. 1 is given by [23]

$$\mathbf{y}_\ell = |\mathbf{F}\mathbf{D}_\ell\mathbf{x}|^2 + \boldsymbol{\omega}_\ell, \quad \ell = 1,\dots,L., \tag{1}$$

where L is the total number of snapshots, $\mathbf{y}_\ell \in \mathbb{R}^n$ represents the acquired measurements, $\boldsymbol{\omega}_\ell$ models the observed noise, $\mathbf{F} \in \mathbb{C}^{n\times n}$ corresponds to the Fourier discrete transformation matrix, $\mathbf{D}_\ell \in \mathbb{C}^{n\times n}$ is a diagonal matrix that represents the coded aperture, $\mathbf{x} \in \mathbb{C}^n$ is the object and $|\cdot|$ represents the pointwise magnitude. Further, defining $\mathbf{y} = [\mathbf{y}_1^T,\dots,\mathbf{y}_L^T]^T \in \mathbb{R}^{m=nL}$, $\boldsymbol{\omega} = [\boldsymbol{\omega}_1^T,\cdots,\boldsymbol{\omega}_L^T]^T \in \mathbb{R}^{m=nL}$, and the matrix $\mathbf{A} = [\mathbf{D}_1\mathbf{F},\dots,\mathbf{D}_L\mathbf{F}]^T$, the quadratic model in (1) can be rewritten as

$$\mathbf{y} = |\mathbf{A}\mathbf{x}|^2 + \boldsymbol{\omega}, \tag{2}$$

where each row of $\mathbf{A}$ is given by $\mathbf{a}_i = \overline{\mathbf{D}}_{r_i}\mathbf{f}_{u_i}$, with $r_i = \lfloor i/n \rfloor + 1$, $u_i = (i-1) \mod n + 1$, and $\mathbf{f}_{u_i}$ the rows of $\mathbf{F}$, for $i = 1,\dots,m$, with $m = nL$. It is worth clarifying that the entries of each matrix $\mathbf{D}_\ell$ are $i.i.d.$ copies of an admissible random variable d, obeying $|d| \leq 1$ [27]. For instance, a variable d uniformly taking random values in the set $\{1,-1,j,-j\}$ is an example of an admissible random variable, which has been previously used in the state-of-the-art [19, 16]. Thus, from (2), each acquired measurement is modeled as

$$(\mathbf{y})_i = |\langle \mathbf{a}_i, \mathbf{x}\rangle|^2 + (\boldsymbol{\omega})_i, \quad i = 1,\dots,m. \tag{3}$$

Considering the illustrated system in Fig. 1 and the acquisition model in (3), this work develops a single-shot 3D shape estimation technique using the optical phase of the object from CDP. This approach is explained in the following section. It is worth mentioning that the state-of-the-art has not explicitly reported a method to estimate the 3D shape of an object from a single-shot of CDP.

3D Object Shape Estimation

This section describes the proposed 3D object shape estimation. The methodology performs a fast estimation to ease the computational complexity of a complete approach, and it is composed by two stages: (i) a fast optical phase estimation strategy from CDP, and (ii) a procedure to estimate the shape of an object using its optical phase.

Step1: Fast Optical Phase Estimation

The proposed phase estimation strategy exploits the mathematical model of CDP in (3) and the sparsity property of natural scenes in the Fourier domain. Specifically, from the imaging literature, it is known that an image can be represented using a few coefficients in the Fourier domain [28, 29]. This implies that the scene of interest $\mathbf{x}$ can be sparsely approximated by a few number of Fourier coefficients, i.e., $\|\theta\|_0 = s \ll n$ where $\|\cdot\|_0$ represents the ℓ_0 pseudo-norm that returns the number of non-zero elements of a given vector, and $\theta = \mathbf{F}\mathbf{x}$. Considering this sparsity prior over the scene $\mathbf{x}$, and the model in (3), the support of θ can be estimated from the CDP [30]. Specifically, define the sample average as,

$$\hat{Z}_p = \frac{1}{m}\sum_{i=1}^{m}(\mathbf{y})_i(\mathbf{B})_{i,p}, \quad p = 1,\dots,n., \tag{4}$$

where $\mathbf{B} = \mathbf{A}\mathbf{F}$, and the expected value of the random variable $\hat{Z}_p$ is given by

$$\mathbb{E}[\hat{Z}_p] \geq c_1\|\mathbf{x}\|_2^2 + c_2|(\theta)_p|^2 + c_3, \tag{5}$$

where c_1, c_2 and c_3 are constants. Then, given the fact that θ is sparse, it is clear that as long as the constant c_2 is sufficiently large, the non-zero coefficients of θ can be exactly recovered. In fact, appealing to the strong law of large numbers, the sample average $\hat{Z}_p \to \mathbb{E}[\hat{Z}_p]$ as m increases, approaches the support of θ and it is estimated as [30, Lemma 1]

$$\mathscr{S} := \left\{1 \leq p \leq n | \text{indices of top-s intances in } \{\hat{Z}_p\}_{p=1}^n\right\}. \tag{6}$$

Once the set $\mathscr{S}$ is estimated following (6), the non-zero entries of θ are approximated solving the following optimization problem [30]

$$\hat{\theta}_{\mathscr{S}} = \underset{\|\theta_{\mathscr{S}}\|_2=1}{\arg\max} \ \theta_{\mathscr{S}}^H \left(\frac{1}{|\mathscr{I}_0|} \sum_{i \in \mathscr{I}_0} \frac{\mathbf{b}_{i,\mathscr{S}} \mathbf{b}_{i,\mathscr{S}}^H}{\|\mathbf{b}_{i,\mathscr{S}}\|_2^2} \right) \theta_{\mathscr{S}}, \tag{7}$$

where $\mathbf{b}_{i,\mathscr{S}}$ is the i-th row of matrix $\mathbf{B}$ which includes the p-th entry $(\mathbf{b}_i)_p$ of $\mathbf{b}_i$ if and only if $p \in \mathscr{S}$. Likewise, for $\theta_{\mathscr{S}}, \hat{\theta}_{\mathscr{S}} \in \mathbb{C}^s$, and $\mathscr{I}_0 \subset \{1,\ldots,nL\}$ is the collection of indices corresponding to the $\lfloor m/6 \rfloor$ largest values of $\{(\mathbf{y})_i / \|\mathbf{a}_i\|_2\}$ [27]. The optimization problem in (7) mathematically involves the estimation of the leading eigenvector of the matrix $\mathbf{Y}_0 := \frac{1}{|\mathscr{I}_0|} \sum_{i \in \mathscr{I}_0} \frac{\mathbf{b}_{i,\mathscr{S}} \mathbf{b}_{i,\mathscr{S}}^H}{\|\mathbf{b}_{i,\mathscr{S}}\|_2^2}$ [30]. Usually, (7) is numerically solved via the power iteration method [31, 20, 19]. This method consists in recursively performing a matrix-vector multiplication between $\mathbf{Y}_0$ and the iterative estimation of the scene [20]. Subsequently, a s-sparse n-dimensional estimation $\hat{\theta}$ is reconstructed by zero-padding $\hat{\theta}_{\mathscr{S}}$ at entries with indices not belonging to $\mathscr{S}$. Thus, since $\hat{\theta}$ is an estimation of the sparse representation of $\mathbf{x}$ in the Fourier domain, $\hat{\mathbf{z}} = \mathbf{F}^H \hat{\theta}$ approximates the scene $\mathbf{x}$. It is worth mentioning that $\hat{\mathbf{z}}$ is a complex vector that approximates both the magnitude and phase of the scene. In summary, Theorem 1 in [30], states that $\hat{\mathbf{z}}$ is a close approximation of the scene $\mathbf{x}$ with high probability.

Theorem 1 *([30, Theorem 1]) Consider noiseless measurements* $(\mathbf{y})_i = |\langle \mathbf{a}_i, \mathbf{x} \rangle|^2$. *Then, with probability of at least* $1 - 2e^{-Cn}$ *for some constant* $C > 0$, *the vector* $\hat{\mathbf{z}}$ *satisfies*

$$\operatorname{dist}(\hat{\mathbf{z}}, \mathbf{x}) \leq \rho \|\mathbf{x}\|_2, \tag{8}$$

for some constant $\rho \in (0,1)$, *provided that* $m \geq \kappa s$, *for* $\kappa > 0$.

The main drawback of the above traditional estimation strategy (6) is the computational complexity. To alleviate this limitation, a modified version is introduced, a fast estimation of the scene from CDP without full reconstruction. This modification is motivated by the fact that the complexity to estimate the non-zero frequencies in (6) is $\mathscr{O}(n^2)$, since $\hat{Z}_p$ in (4) is obtained performing matrix-vector multiplications. To reduce the computational complexity of this step, (6) is equivalently performed in this work with a low-pass filter. Mathematically, the effect of this filter is the selection of the most representative low frequencies of the scene in the Fourier domain. Additionally, it is well-known that filtering a scene can be rapidly performed through the fast Fourier transform with a computational complexity of $\mathscr{O}(n\log(n))$ [32], which is substantially lower than $\mathscr{O}(n^2)$. The proposed estimation method also follows a power iteration methodology summarized in Algorithm 1. Observe that this method requires the sampling vectors, the acquired CDP, and a low-pass filter $\mathscr{G}$. Among different filter types, e.g., Gaussian, Butterworth, and Chebyshev [32], this work employs a Gaussian filter to illustrate the effectiveness of Algorithm 1, but any other filter could be used.

Algorithm 1 Fast Optical Phase Estimation

1: **Input:** Acquired data $\{(\mathbf{a}_i;(\mathbf{y})_i)\}_{i=1}^m$, maximum number of iterations T, and low pass filter $\mathscr{G}$.
2: $\tilde{\mathbf{z}}^{(0)} \leftarrow$ Chosen randomly.
3: **Set** $\mathscr{I}_0$ as the set of indices corresponding to the $\lfloor m/6 \rfloor$ largest values of $\{(\mathbf{y})_i / \|\mathbf{a}_i\|_2\}$.
4:

$$\mathbf{Y}_0 := \frac{1}{|\mathscr{I}_0|} \sum_{i \in \mathscr{I}_0} \frac{\mathbf{b}_{i,\mathscr{S}} \mathbf{b}_{i,\mathscr{S}}^H}{\|\mathbf{b}_{i,\mathscr{S}}\|_2^2}$$

5: **for** $t = 0 : T-1$ **do**
6: $\quad \grave{\mathbf{z}}^{(t+1)} \leftarrow \mathscr{G}\left(\mathbf{Y}_0 \tilde{\mathbf{z}}^{(t)}\right)$
7: $\quad \tilde{\mathbf{z}}^{(t+1)} \leftarrow \frac{\grave{\mathbf{z}}^{(t+1)}}{\left\|\grave{\mathbf{z}}^{(t+1)}\right\|_2}$
8: **end forend for**
9: Compute $\hat{\mathbf{z}} = \sqrt{\frac{\sum_{i=1}^m (\mathbf{y})_i}{m}} \tilde{\mathbf{z}}^{(T)}$
10: **Return:** $\hat{\mathbf{z}}$

Following the iteration process, the characteristic matrix-vector multiplication of the power iteration method $\mathbf{Y}_0 \tilde{\mathbf{z}}^{(t)}$ is performed in line 6. The result of this product is considered the current estimation of both the magnitude and phase of the scene. Also, in line 6, a low-pass filtering process over $\mathbf{Y}_0 \tilde{\mathbf{z}}^{(t)}$ is accomplished, where $\mathscr{G}$ represents the filter. The effect of iteratively applying $\mathscr{G}$ over the estimation of the image is the selection of those low-frequencies that sparsely represent the image in the Fourier domain. Observe that this selection is rapidly performed in comparison with (6) [32]. Finally, Algorithm 1 returns the scaled complex vector $\hat{\mathbf{z}}$, which, according to Theorem 1 is a close approximation of both the magnitude and phase of the scene. The scaling factor $\sqrt{\frac{\sum_{i=1}^m (\mathbf{y})_i}{m}}$ in line 9 is a close approximation of $\|\mathbf{x}\|_2$ [20] and it has to be calculated because $\tilde{\mathbf{z}}$ is a unitary image.

Step 2: 3D Object Shape

Considering the output of Algorithm 1, this section describes a procedure to estimate the shape of the object. To that end, remark the Euler's formula, $\hat{\mathbf{z}} = \mathbf{r} \odot e^{j\varphi}$, where $\mathbf{r}$ and φ are the magnitude and phase of $\hat{\mathbf{z}}$, and $\odot$ denotes the Hadamard product. Then, to estimate the 3D object shape, the unwrapped version of the phase information φ is used [33]. The unwrapping process is needed since the *arctan* function induces discontinuities at 2π, which is mathematically given as

$$\varphi_{unwrapp} = \varphi + 2k\pi, \tag{9}$$

where k is an integer representing the projection period [33]. It is important mentioning that the unwrapping methods only provide a relative unwrapping and do not solve the absolute phase. The depth coordinate can be calculated based on the difference between measured phase $\varphi_{unwrapp}$ and the phase value from a reference plane [34]. This reference plane is obtained from the calibration process of the acquisition system [33]. Thus, mathematically the depth coordinate of the 3D object is determined as

$$\mathbf{p} = c_0 + c_1(\varphi_{unwrapp} - \varphi_0), \tag{10}$$

where φ_0 is the reference phase and c_0, c_1 are tunable constants. Particularly, for this work these constant are fixed as $c_0 = 200$ and $c_1 = 5$. To summarize the proposed 3D object shape method Algorithm 2 is introduced.

Algorithm 2 3D Object Shape

1: **Input:** data $\{(\mathbf{a}_i;(\mathbf{y})_i)\}_{i=1}^{m}$, the constants c_0, c_1, and the reference phase φ_0.
2: $\hat{\mathbf{z}} \leftarrow$ Algorithm 1$(\mathbf{a}_i;\mathbf{y})$.
3: $\hat{\mathbf{z}} = \mathbf{r} \odot e^{j\varphi}$
4: $\varphi_{unwrapp} = \varphi + 2k\pi$
5: $\mathbf{p} = c_0 + c_1(\varphi_{unwrapp} - \varphi_0)$
6: **Return:** $\mathbf{p}$

Numerical Simulations

The performance of Algorithms 1 and 2 are evaluated under noiseless and noisy scenarios. For the noisy cases, the signal-to-noise ratio (SNR) is defined as $\text{SNR} = 10\log(\|\mathbf{y}\|_2^2/(m\sigma^2))$, with σ^2 as the variance of the noise. Particularly, Algorithm 1 is compared to its alternatives: orthogonality-promoting initialization [19] (OPI), weighted maximal correlation initialization [20] (WMCI), and truncated spectral initialization [21] (TSI). Additionally, the results of Algorithm 2 are compared with the 3D object shape reconstruction using a structured light system. This system was accomplished by implementing a phase shift structured light setup through three coded sinusoidal striped patterns with phase shifts 0, $\pi/2$, and π [35], as shown in Fig. 2. The discrete random variable d used for all the experiments to build $\mathbf{D}_\ell$ uniformly takes values in the set $\{j,-j,1,-1\}$ that trivially satisfy $|d| \leq 1$. All tested experiments were obtained by averaging 100 runs.[1].

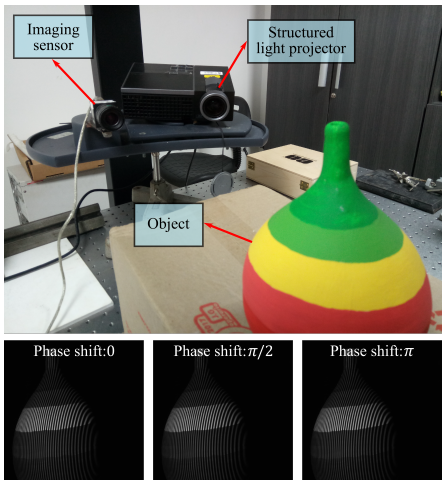

Figure 2. *Structured light system using three coded sinusoidal stripes with phase shift 0, $\pi/2$ and π [36]. The light projector illuminates the 3D object with a coded sinusoidal stripe that allows determining its optical phase.*

Optical Phase Estimation Accuracy

In this section, the performance of Algorithm 1, to estimate the optical phase of the object, is compared against some traditional estimation methods such as OPI [19], WMCI [20] and TSI [21] for different SNR levels. For this test, the maximum number of iterations T of Algorithm 1 is fixed as $T = 200$. The results are summarized in Fig. 3. From these results, it can be noticed that Algorithm 1 outperforms its competitive alternatives since it returns a closer estimation of the optical phase using 75% fewer measurements compared to WMCI, and 86% fewer measurements compared to OPI and TSI. These results demonstrate the effectiveness of Algorithm 1 to estimate the optical phase of the object accurately.

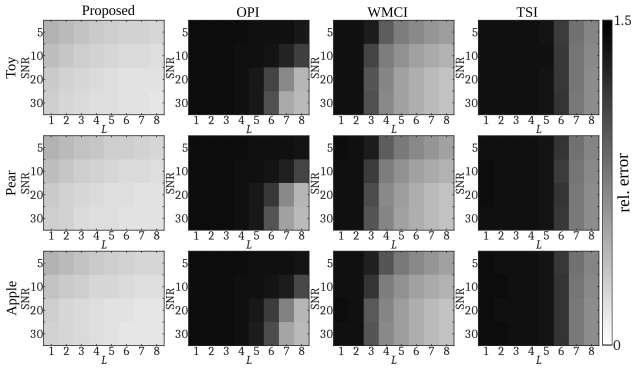

Figure 3. *Relative errors using different estimation strategies, noise levels, and number of snapshots. A lighter color indicates a closer estimate of the scene.*

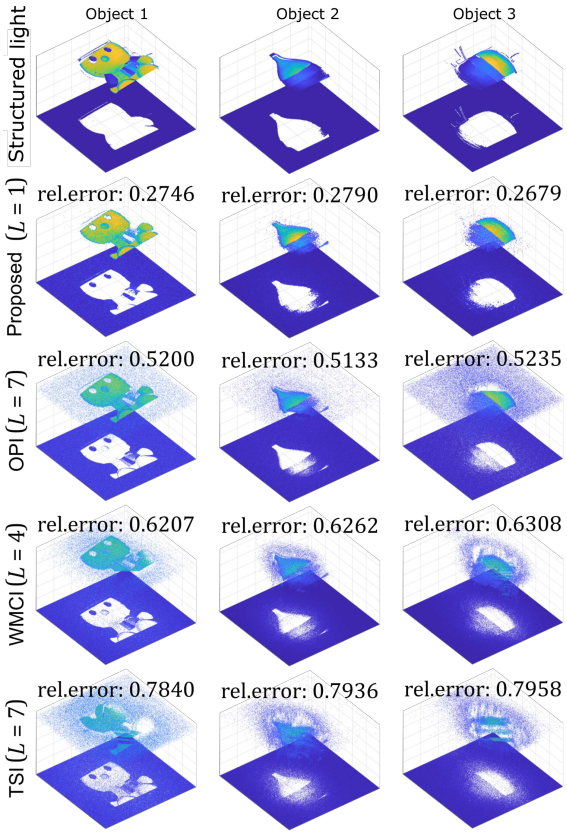

Figure 4. *3D objects shape estimation using Algorithm 2, OPI, WMCI and TSI approaches with number of snapshots $L = 1$, $L = 7$, $L = 4$, and $L = 7$, respectively, and $\text{SNR} = 30[\text{dB}]$.*

[1]The experiments were carried out using Matlab 2017b on a desktop computer with an Intel(R) core(TM) i7-6700 CPU 3.40 GHz processor and 32 GB RAM memory. The code of the proposed methodology is available at `http://diffraction.uis.edu.co/codes.html`

3D Object Shape Estimation

In this section, the performance of Algorithm 2 is compared against a structured light strategy, considered as the ideal estimation, and the 3D shape estimates from the obtained phase using some traditional estimation methods such as OPI [19], WMCI [20] and TSI [21] for SNR=30dB. Three objects were analyzed. The results are summarized in Fig. 4. From these results, it can be noticed that Algorithm 2 outperforms the competitive alternatives since it returns a closer estimation of the 3D object shape using 75% fewer measurements compared to WMCI, and 86% fewer measurements compared to OPI and TSI. Note that the competitive alternatives of Algorithm 2 require more than one snapshot to estimate the 3D surface, as shown in Fig. 4, then this experiment illustrates estimation results obtained by using the minimum number of snapshots according to each estimation strategy. Finally, these results also suggest that Algorithm 2 returns an accurate estimation of the 3D surface using 60% fewer measurements compared to a structured light methodology, without involving a full time demanding reconstruction of the optical phase.

Conclusions

A 3D object shape estimation methodology based on CDP was presented. This method is composed of two stages: first, an estimation of the optical of the object, second, a procedure to estimate the shape of an object using its optical phase. Simulation results show that the proposed 3D object shape methodology can accurately estimate the shape of a 3D object using a single snapshot, even in highly noisy scenarios. In fact, from the numerical tests, it can be concluded that the proposed method requires up to 75% fewer measurements to better estimate the 3D object shape than competitive alternatives. Future work includes implementing the proposed 3D object shape method on real data to validate its performance. Another interesting research direction would be to examine similar strategies for 3D object shape estimation in real-time.

Acknowledgments

This work was supported by Vicerrectoría de Investigación y Extensión VIE-UIS (2486), and Colciencias-Programa de estancias postdoctorales (811-2018).

References

[1] A. L. Holsteen, D. Lin, I. Kauvar, G. Wetzstein, and M. L. Brongersma, "A light-field metasurface for high-resolution single-particle tracking," *Nano letters*, vol. 19, no. 4, pp. 2267–2271, 2019.

[2] F. Willomitzer and G. Häusler, "Single-shot 3d motion picture camera with a dense point cloud," *Optics express*, vol. 25, no. 19, pp. 23451–23464, 2017.

[3] H. Jin, A. J. Yezzi, Y.-H. Tsai, L.-T. Cheng, and S. Soatto, "Estimation of 3d surface shape and smooth radiance from 2d images: A level set approach," *Journal of Scientific Computing*, vol. 19, no. 1-3, pp. 267–292, 2003.

[4] S. Heist, C. Zhang, K. Reichwald, P. Kühmstedt, G. Notni, and A. Tünnermann, "5d hyperspectral imaging: fast and accurate measurement of surface shape and spectral characteristics using structured light," *Optics express*, vol. 26, no. 18, pp. 23366–23379, 2018.

[5] A. Gruen and D. Akca, "Least squares 3d surface and curve matching," *ISPRS Journal of Photogrammetry and Remote Sensing*, vol. 59, no. 3, pp. 151–174, 2005.

[6] V. Couture, N. Martin, and S. Roy, "Unstructured light scanning to overcome interreflections," in *2011 International Conference on Computer Vision*, pp. 1895–1902, IEEE, 2011.

[7] M. Gupta and S. K. Nayar, "Micro phase shifting," in *2012 IEEE Conference on Computer Vision and Pattern Recognition*, pp. 813–820, IEEE, 2012.

[8] T. Weise, B. Leibe, and L. Van Gool, "Fast 3d scanning with automatic motion compensation," in *2007 IEEE Conference on Computer Vision and Pattern Recognition*, pp. 1–8, IEEE, 2007.

[9] H. Kawasaki, R. Furukawa, R. Sagawa, and Y. Yagi, "Dynamic scene shape reconstruction using a single structured light pattern," in *2008 IEEE conference on computer vision and pattern recognition*, pp. 1–8, Ieee, 2008.

[10] A. O. Ulusoy, F. Calakli, and G. Taubin, "One-shot scanning using de bruijn spaced grids," in *2009 IEEE 12th International Conference on Computer Vision Workshops, ICCV Workshops*, pp. 1786–1792, IEEE, 2009.

[11] J. Bacca, S. Pinilla, and H. Arguello, "Super-resolution phase retrieval from designed coded diffraction patterns," *IEEE Transactions on Image Processing*, 2019.

[12] S. Pinilla, J. Poveda, and H. Arguello, "Coded diffraction system in x-ray crystallography using a boolean phase coded aperture approximation," *Opt. Comm.*, vol. 410, pp. 707–716, 2018.

[13] E. J. Candes, X. Li, and M. Soltanolkotabi, "Phase retrieval from coded diffraction patterns," *Applied and Computational Harmonic Analysis*, vol. 39, no. 2, pp. 277–299, 2015.

[14] P. Netrapalli, P. Jain, and S. Sanghavi, "Phase retrieval using alternating minimization," in *Adv. in Neu. Inf. Proc. Sys.*, pp. 2796–2804, 2013.

[15] E. J. Candes, T. Strohmer, and V. Voroninski, "Phaselift: Exact and stable signal recovery from magnitude measurements via convex programming," *Comm. on Pure and App. Math.*, vol. 66, no. 8, pp. 1241–1274, 2013.

[16] S. Pinilla, J. Bacca, and H. Arguello, "Phase retrieval algorithm via nonconvex minimization using a smoothing function," *IEEE Trans. on Signal Proc.*, vol. 66, no. 17, pp. 4574–4584, 2018.

[17] Y. Shechtman, Y. C. Eldar, A. Szameit, and M. Segev, "Sparsity based sub-wavelength imaging with partially incoherent light via quadratic compressed sensing," *Opt. exp.*, vol. 19, no. 16, pp. 14807–14822, 2011.

[18] Z. Yuan, Q. Wang, and H. Wang, "Phase retrieval via sparse wirtinger flow," *arXiv preprint arXiv:1704.03286*, 2017.

[19] G. Wang, G. B. Giannakis, and Y. C. Eldar, "Solving systems of random quadratic equations via truncated amplitude flow," *IEEE Trans. on Inf. The.*, vol. 64, no. 2, pp. 773–794, 2018.

[20] G. Wang, G. B. Giannakis, Y. Saad, and J. Chen, "Phase retrieval via reweighted amplitude flow," *IEEE Trans. on Signal Proc.*, vol. 66, no. 11, pp. 2818–2833, 2018.

[21] Y. Chen and E. Candes, "Solving random quadratic systems of equations is nearly as easy as solving linear systems," in *Adv. in Neu. Inf. Proc. Sys.*, pp. 739–747, 2015.

[22] P. M. Pardalos and S. A. Vavasis, "Quadratic programming

with one negative eigenvalue is np-hard," *J. of Gl. Opt.*, vol. 1, no. 1, pp. 15–22, 1991.
[23] E. J. Candes, X. Li, and M. Soltanolkotabi, "Phase retrieval from coded diffraction patterns," *App. and Comp. Harm. Anal.*, vol. 39, no. 2, pp. 277–299, 2015.
[24] E. G. Loewen and E. Popov, *Diffraction gratings and applications*. CRC Press, 2018.
[25] J. M. Rodenburg, "Ptychography and related diffractive imaging methods," *Ad. in imag. and elev. phys.*, vol. 150, pp. 87–184, 2008.
[26] P. Thibault, M. Dierolf, O. Bunk, A. Menzel, and F. Pfeiffer, "Probe retrieval in ptychographic coherent diffractive imaging," *Ultramicroscopy*, vol. 109, no. 4, pp. 338–343, 2009.
[27] A. Guerrero, S. Pinilla, and H. Arguello, "Phase recovery from designed coded diffraction patterns in optical imaging," *IEEE tran. on image proc.*, vol. (In revision).
[28] J. R. Jensen and K. Lulla, "Introductory digital image processing: a remote sensing perspective," 1987.
[29] D. Taubman and M. Marcellin, *JPEG2000 image compression fundamentals, standards and practice: image compression fundamentals, standards and practice*, vol. 642. Springer Science & Business Media, 2012.
[30] G. Wang, L. Zhang, G. B. Giannakis, M. Akçakaya, and J. Chen, "Sparse phase retrieval via truncated amplitude flow," *IEEE Trans. on Signal Proc.*, vol. 66, no. 2, pp. 479–491, 2017.
[31] Y. Saad, *Iterative methods for sparse linear systems*, vol. 82. siam, 2003.
[32] R. C. Gonzalez and P. Wintz, "Digital image processing(book)," *Reading, Mass., Addison-Wesley Publishing Co., Inc.(Applied Mathematics and Computation*, no. 13, p. 451, 1977.
[33] J. Geng, "Structured-light 3d surface imaging: a tutorial," *Advances in Optics and Photonics*, vol. 3, no. 2, pp. 128–160, 2011.
[34] H. Sagan, *Space-filling curves*. Springer Science & Business Media, 2012.
[35] S. Zhang, *High-Speed 3D imaging with digital fringe projection techniques*. CRC Press, 2016.
[36] E. Díaz, J. Meneses, and H. Arguello, "Hyperspectral+ depth imaging using compressive sensing and structured light," in *3D Im. Acq. and Dis.: Tech., Perc. and App.*, pp. 3M3G–6, Optical Society of America, 2018.

Author Biography

Samuel Pinilla received the B.S. degree in computer science, in 2014, from the Universidad Industrial de Santander, Bucaramanga, Colombia, where he is currently working towards the Ph.D. degree at the Department of Electrical and Computer Engineering. His research interests include high-dimensional structured signal processing and non-convex optimization methods.

Author Biography

Laura Galvis Received the B.Sc. and M.Sc. degrees in computer science from the Universidad Industrial de Santander (UIS), Colombia, in 2009 and 2012, respectively, and the Ph.D. degree in electrical and computer engineering from the University of Delaware (UDEL), Newark, DE, USA, in 2018. She is currently a postdoctoral researcher at UIS, sponsored by Colciencias and UIS. Her main research areas are computational optical imaging, compressive sensing, and high-dimensional signal processing.

Author Biography

Karen Egiazarian received a Ph.D. degree in physics and mathematics from Moscow State University, Moscow, Russia, in 1986, and the D.Tech. degree from the Tampere University of Technology (TUT), Finland, in 1994. Since 1996, he has been an Assistant Professor with the Institute of Signal Processing, TUT, where he is currently a Professor, leading the Transforms and Spectral Methods Group. His research interests are in the areas of applied mathematics, signal processing, and digital logic.

Author Biography

Henry Arguello received the Masters degree in electrical engineering from the Universidad Industrial de Santander, Bucaramanga, Colombia, and the Ph.D. degree from the Electrical and Computer Engineering Department, University of Delaware, Newark, DE, USA in 2003 and 2013, respectively. He is currently a Titular Professor at the Computer Science Department, Universidad Industrial de Santander. His research interests include statistical signal processing, high-dimensional signal coding and processing, optical imaging, optical code design, and computational imaging.

JOIN US AT THE NEXT EI!

IS&T International Symposium on

Electronic Imaging

SCIENCE AND TECHNOLOGY

Imaging across applications . . . Where industry and academia meet!

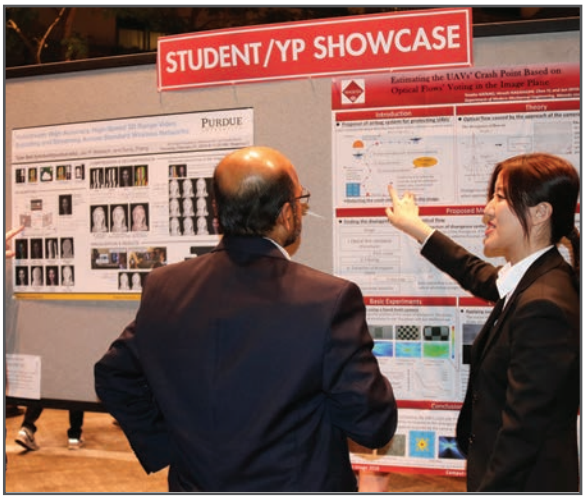

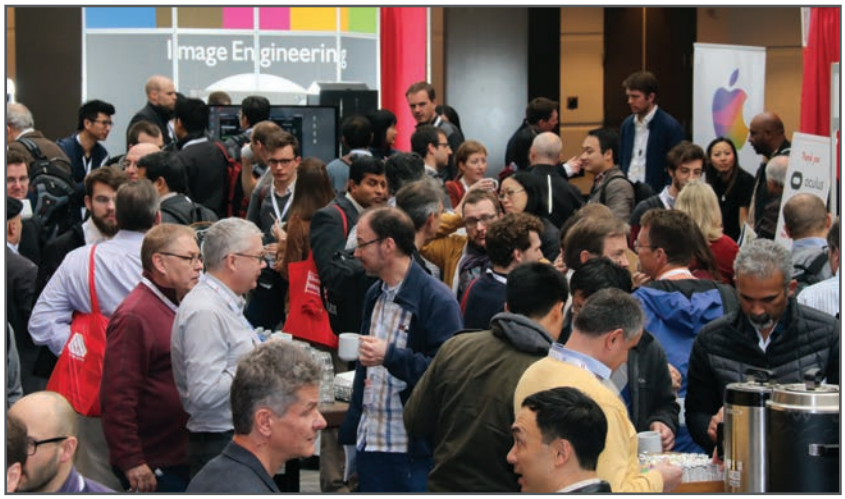

• SHORT COURSES • EXHIBITS • DEMONSTRATION SESSION • PLENARY TALKS •
• INTERACTIVE PAPER SESSION • SPECIAL EVENTS • TECHNICAL SESSIONS •

www.electronicimaging.org

IS&T
imaging.org